J Herbmed Pharmacol. 2022; 11(1): 114-120.

JHP

http://www.herbmedpharmacol.com

doi: 10.34172/jhp.2022.13

Journal of Herbmed Pharmacology

Preparation of chelidonine highly loaded poly(lactide-co-glycolide)-based nanoparticles using a single emulsion method: Cytotoxic effect on MDA-MB-231 cell line

Zahra Hamidia[1], Kahin Shahanipour[1*], Nasrin Talebian[2], Ramesh Monajemi[3]

[1]Department of Biochemistry, Falavarjan Branch, Islamic Azad University, Isfahan, Iran
[2]Department of Chemistry, Shahreza Branch, Islamic Azad University, Shahreza, Iran
[3]Department of Biology, Falavarjan Branch, Islamic Azad University, Isfahan, Iran

ARTICLE INFO

Article Type:
Original Article

Article History:
Received: 10 June 2021
Accepted: 27 October 2021

Keywords:
Chelidonium majus
Bioavailability
Nanoparticles
Drug delivery
Herbal drug
Breast cancer

ABSTRACT

Introduction: Chelidonine, a bio-active component of *Chelidonium majus*, has been investigated for its anti-proliferative effects on various cancer cell lines with multidrug resistance (MDR). Although the results are auspicious, its poor water solubility and low bioavailability are the main limitations for clinical applications. This study aimed to develop poly(lactic-co-glycolic acid) (PLGA) nanoparticles loaded with chelidonine, in order to enhance its bioavailability for oral administration and improve the therapeutic index.
Methods: Herein, we encapsulated chelidonine in PLGA nanoparticles using a single emulsion solvent evaporation method. Nanoparticles were characterized in terms of size, surface charge and morphology, encapsulation efficiency, drug loading, and in vitro drug release profile. The anti-cancer efficacy of chelidonine-loaded nanoparticles and free chelidonine was evaluated in MDA-MB-231 breast cancer cells.
Results: The physicochemical characteristics showed spherical particles in nanometer size range (263 ± 19.6 nm), with negative surface charge (–20.67 ± 2.48 mv), high encapsulation efficiency (76.53 ± 3.61%), and drug loading (22.47 ± 0.09%), as well as drug release amount of 60.27±5.68% up to 10 days. Furthermore, chelidonine-loaded nanoformulations were found to improve anti-cancer potential, compared with unentrapped chelidonine.
Conclusion: This *in vitro* study showed that the encapsulation of chelidonine, as a potent herbal drug, in a polymeric matrix enhances its bioavailability. This offers an efficient vehicle for targeted drug delivery in cancer treatment.

Implication for health policy/practice/research/medical education:
This study revealed that encapsulation of chelidonine in PLGA nanoparticles led to a higher cytotoxic effect on MDA-MB-231 cancer cells, in comparison with free chelidonine, which offers a potential therapeutic approach for cancer treatment in the future.

Please cite this paper as: Hamidia Z, Shahanipour K, Talebian N, Monajemi R. Preparation of chelidonine highly loaded poly(lactide-co-glycolide)-based nanoparticles using a single emulsion method: Cytotoxic effect on MDA-MB-231 cell line. J Herbmed Pharmacol. 2022;11(1):114-120. doi: 10.34172/jhp.2022.13.

Introduction

Breast cancer is considered the second mortality cause in women worldwide (1). Surgery, chemotherapy, radiation, immunotherapy, and hormone therapy are the main tools of treatment showing adverse effects (2). Conventional chemotherapy bears side effects due to non-specific action and multidrug resistance (MDR) (3). To overcome this problem, various anti-cancer agents derived from plants are available for clinical use due to their diverse functions and minimal side effects to normal tissues (4).

Chelidonium majus, also known as greater celandine, is widely distributed in Asia and Europe. It is an official drug in several pharmacopeias (5). Various parts of the crude extract have been reported to exhibit biological activities, such as immunomodulatory, antimicrobial, antiviral, anti-cancer, and anti-inflammatory properties (6). Chelidonine, a benzophenanthridine alkaloid of *C. majus* has indicated promising anti-proliferative potentials against several cancer cells (7). However, systemic bioavailability restricts its application for oral

***Corresponding author**: Kahin Shahanipour,
Email: shahanipur_k@yahoo.com

administration (8). Nanoparticulated-drug delivery systems have been widely used in order to deliver anti-cancer agents into tumors. Poly(lactic-co-glycolic acid) (PLGA) has received great attention as a FDA-approved polymer due to its ability to carry hydrophobic drugs, biodegradability, biocompatibility as well as controlled drug release profile (9). PLGA nanoparticles (NPs) accumulate in tumor sites through enhanced permeation and retention (EPR) effect (10). PLGA, as a biodegradable polymer, is hydrolyzed to final degradation monomeric products, lactic and glycolic acids, which are eliminated by the Krebs cycle (11). Therefore, the purposes of the current research were to develop a PLGA-based drug delivery system to enhance the therapeutic potential of chelidonine, evaluate the physicochemical properties of NPs and drug release profiles, and investigate the anti-cancer potential of nano-formulations in MDA-MB-231 cells, as the laboratory model for breast cancer.

Materials and Methods

Materials

PLGA with a 50:50 monomer ratio (ester-terminated, MW 24 000-38 000; inherent viscosity 0.32-0.44 dL/g at 30ºC) and chelidonine (97.0% HPLC grade) were purchased from Sigma-Aldrich, USA. Poly-vinyl-alcohol (PVA, Mw 60 000) was purchased from TITRACHEM, Iran. A breast cancer cell line (MDA-MB-231) was obtained from Pasteur Institute, Iran. MTT was purchased from Sigma-Aldrich. HPLC grade Ethyl acetate (EA) and dimethyl sulfoxide (DMSO) were purchased from Merck, Germany.

Preparation of chelidonine-loaded NPs

Chelidonine-loaded PLGA (CM-PLGA) NPs were prepared via single emulsion solvent evaporation method (12). Briefly, 20 mg PLGA and 5 mg chelidonine were dissolved in 1 mL ethyl acetate. This organic phase solution was added to 10 ml of 4% PVA solution (aqueous phase) under constant vortex (MSV-2, KIAGEN, Iran) and emulsified in an ice bath for 3 minutes using a microtip ultrasonic probe in the pulsed manner (70% intensity, UIP 1000hd, Hielscher, Germany) to form the emulsion (w/o). The emulsion was then left on a magnetic stirrer at room temperature for 2 hours to evaporate the solvent. The NPs were collected by centrifuging at 17 000 rpm for 20 minutes (Sigma 3K30, Sigma, Germany). The supernatant containing free drug was discarded for further analysis and the pellet was washed 2-3 times with deionized water and lyophilized (VaCo5, Zirbus, Germany) for 48 hours to get a fine powder of NPs. Blank NPs were prepared using the same procedure without adding chelidonine.

Physicochemical characterization of NPs

Size distribution and surface charge

Hydrodynamic diameter and polydispersity index (PDI) of NPs were determined using dynamic light scattering (VASCO Particle Size Analyzer, France). Freshly nanoparticle suspension (1 mg/mL) was prepared and sonicated for 30 s. The analysis was performed at a scattering angle of 90°. Diluted nanoparticle suspension, as described above, was used to measure the zeta potential of NPs using Zetasizer (SZ-100 Nanoparticle Analyzer). An average of three determinations was reported.

Drug loading (DL) and encapsulation efficiency (EE)

The free chelidonine (FCM) amount was determined using the supernatant obtained after nanoparticle production. Various concentrations of standard chelidonine solution (0.01-2 mg/mL) were prepared, and the standard calibration curve was drawn from the UV absorbance values at 290 nm (correlation coefficient of $r^2>0.998$) using a UV-visible spectrophotometer (JENWAY 7315 UV/Visible Spectrophotometer). The measurements were done in triplicate. Encapsulation efficiency (EE) and drug loading (DL) were calculated as below:

$$EE(\%) = \frac{[total\ chelidonine] - [free\ chelidonine]}{[total\ chelidonine]} \times 100$$

$$DL(\%) = \frac{[total\ chelidonine] - [free\ chelidonine]}{[polymer]} \times 100$$

Field emission scanning electron microscopy

To evaluate the surface morphology, field emission scanning electron microscopy (FE-SEM) (Philips XL30, Netherlands) was used. The lyophilized NPs were coated with gold and were analyzed at an accelerating voltage of 5 kV under vacuum.

Transmission electron microscopy

To evaluate the internal structure of NPs, TEM (JEOL, Tokyo, Japan) was used. A drop of NPs suspension was placed on a carbon-coated copper transmission electron microscopy (TEM) grid and allowed to air-dry. The dried samples were then examined at 120 kV under a microscope.

Fourier transform infrared spectroscopy

In the Fourier transform infrared (FTIR) spectroscopic study, FCM, blank PLGA NPs, and CM-PLGA NPs were scanned over a wavenumber range of 4000–400 cm^{-1} in an FTIR spectrophotometer (Perkin Elmer 65, USA) to understand the possible chemical interactions occurring between the drug and the polymer matrix.

X-ray diffraction study

To determine the crystalline and amorphous nature of chelidonine before and after encapsulation into the PLGA NPs, X-ray diffraction (XRD) patterns of FCM, PLGA NPs, and CM-PLGA NPs were measured. The experiment was performed by a D/Max– B Rikagu diffractometer (AW-XDM300, UK). All experiments were performed at room temperature.

Long-term stability study

To assess the stability of chelidonine-loaded NPs prepared by a single emulsion method, these were stored at 25°C away from direct light for three months. Samples were analyzed for mean particle size and zeta potential. The experiments were carried out in triplicates.

In vitro drug release

To evaluate the *in vitro* release of chelidonine accurately weighed samples (3 mg) were suspended in 6 mL of phosphate-buffered saline (pH 7.4) and transferred into a pre-swelled dialysis bag (MWCO =12-14 kDa). The dialysis bag was immersed into 30 mL release medium (PBS, pH 7.4) on a shaking incubator (Model: KM C 65, Fan Azma Gostar, Iran) at 100 rpm. At various time intervals within 10 days, 1 mL of the release media was taken out and an equal volume of fresh release media was replaced. The absorbance of each sample was measured by UV–Visible spectrophotometer at a wavelength of 290 nm and chelidonine concentration released from PLGA NPs was determined using a standard calibration curve. The release experiments were performed in triplicate. Data were plotted as the percentage of cumulative drug release versus time.

In vitro cytotoxicity assay

The cytotoxic effects of FCM, blank PLGA NPs, and CM-PLGA NPs on the MDA-MB-231 cell line were analyzed by the MTT assay. Briefly, the cells were plated at a density of 1×10^4 cells per well in 96-well plates and cultivated at 37°C in humidified air containing 5% CO_2 (Heal Force HF-90, JAPAN) for 24 hours. The cells were then treated with various concentrations (50-500 µg/mL) of FCM, PLGA NPs, and CM-PLGA NPs, and incubated for 24, 48, and 72 hours at 37˚C. After a specified incubation time, the culture medium was discarded, and 20 µL of MTT (5 mg/mL) solution was added to each well, and incubation was carried out for 4 hours at 37˚C. The supernatant was withdrawn and 150 µL DMSO was added to each well for dissolving the formazan crystals. The UV absorbance of the solubilized formazan crystals was measured spectrophotometrically at a wavelength of 570 nm using the microplate reader. The experiment was performed in triplicate. The viability of cells was calculated using the following equation:

$$Cell\ viability\,\% = \frac{Abs_{test\ cells}}{Abs_{control\ cells}} \times 100$$

where $Abs_{test\ cells}$ and $Abs_{control\ cells}$ are the amounts of formazan in treated and non-treated cells, respectively.

Statistical Analysis

All results are expressed as mean ± SD. Statistical analysis was carried by one-way ANOVA. P values less than 0.05 were considered statistically significant.

Results

NPs characterization

Chelidonine-encapsulated NPs were prepared with 22.47 ± 0.09% drug loading in the nanometer range and had 76.53 ± 3.61% encapsulation efficiency. DLS measurements showed the mean particle size of 263 ± 19.6 nm with the PDI values of 0.211 ± 0.04 and −20.67 ± 2.48 mv zeta potential for CM-PLGA NPs (Table 1). From the FE-SEM micrograph, the freshly prepared CM-PLGA NPs were spherical in shape with a relatively monodisperse size distribution (Figure 1A). TEM micrographs of the samples showed a spherical shape and smooth surface with a particle size in the nanometric range (Figure 1B). No aggregation or adhesion was observed in microscopic analysis. The smaller particle size obtained by FE-SEM and TEM is probably due to shrinking in the dry state of NPs compared to DLS results. The lyophilized NPs were stored at 25°C for 3 months for particle size measurement. As shown in Table 1, no significant increase was observed in the mean particle size, PDI, as well as zeta potential values after three months' storage, which confirms the stability of prepared nanoformulations.

FTIR spectroscopic study

FTIR analysis was performed in the region of 4000–450 cm^{-1} to determine the interaction between chelidonine and polymeric matrix. As seen in Figure 2, peaks at 3469 cm^{-1} (OH group), 2887 cm^{-1} (C-H stretching of CH_2 and

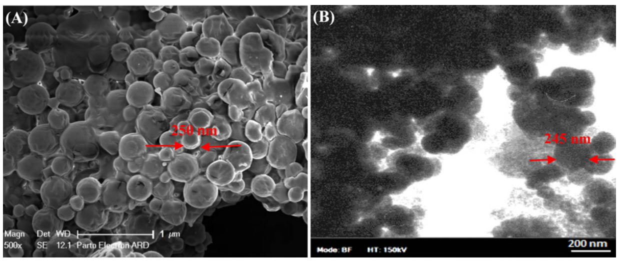

Figure 1. Morphology images for **chelidonine loaded PLGA (CM-PLGA)** NPs; (A) FE-SEM images and (B) TEM images. PLGA: Poly(lactic-co-glycolic acid); NPs: Nanoparticles; CM-PLGA: Chelidonine-loaded PLGA; FE-SEM: Field emission scanning electron microscopy; TEM: Transmission electron microscopy.

Table 1. Stability assessments of chelidonine-loaded PLGA (CM-PLGA) nanoparticles at 4°C for 3 months

Time (month)	Formulation	Mean diameter (nm) ± SD*	PDI ± SD*	Zeta potential (mv) ± SD*
0	CM-PLGA	263 ± 19.6	0.211 ± 0.04	−20.67 ± 2.48
3	CM-PLGA	270 ± 19.6	0.268 ± 0.01	−26.01 ± 3.45

*Data are mean ± SD (n=3); PLGA: Poly(lactic-co-glycolic acid) (PLGA); PDI: polydispersity index.

CH_3 groups), 1760 cm^{-1} (C-O stretching bonds), and 1440 cm^{-1} (C–H bend) were recorded for PLGA NPs (18). The characteristic absorption peaks of FCM exhibited the characteristic peaks at 3370 cm^{-1} attributed to OH group, 2915 cm^{-1}, 2834 cm^{-1}, 2781 cm^{-1} to C–H stretching of CH_2 group, 1651 cm^{-1} to C-O stretching, 1485 cm^{-1} to C-N stretching, and 1345–1029 cm^{-1} to the aromatic group and aliphatic CH_3 group (8). The peak at 3370 cm^{-1} related to –OH was broadened and stretched in CM-PLGA NPs spectra compared with FCM, which is probably due to encapsulation of chelidonine in PLGA NPs. The splitting and broadening of bands at 2900 cm^{-1} and 2825 cm^{-1} may be attributed to C-H stretching of chelidonine and C-H stretching of PLGA in NPs. A new band appearing at 1754 cm^{-1} indicates the C–O–C stretching as the characteristic peak for PLGA NPs. The chelidonine C–O stretching band was also seen at 1642 cm^{-1}.

X-ray diffraction study
XRD pattern shows the crystallography and phases of different nanoparticle formulations (Figure 3). FCM exhibited three distinct peaks at 2θ28.35º, 40.56º, and 50.25º, which reflects that the drug is highly crystalline. No distinct peaks were observed in the XRD pattern of PLGA NPs and CM-PLGA NPs, which indicates their amorphous nature.

In vitro drug release profile
Figure 4 represents the drug release profile of FCM and encapsulated chelidonine. The initial burst release (around 20.35 ± 4.21%) was observed within the first 24 h for CM-PLGA NPs and followed by a slower phase. Approximately, 60.27± 5.68% of chelidonine was released from nanoformulations over a period of 10 days, while this amount was about 38.11± 3.19% for FCM.

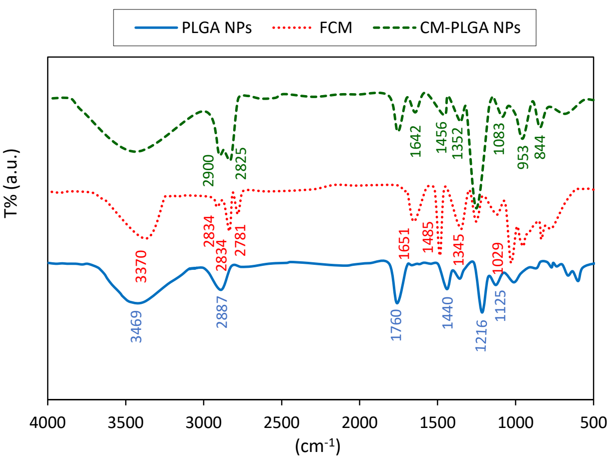

Figure 2. Fourier transform infrared spectra of PLGA NPs, free chelidonine (FCM), and chelidonine loaded PLGA (CM-PLGA) NPs. PLGA: Poly(lactic-co-glycolic acid); NPs: Nanoparticles; CM-PLGA: Chelidonine-loaded PLGA.

In vitro cytotoxicity
In vitro cytotoxic effects of blank PLGA NPs, FCM, and CM-PLGA NPs were performed by MTT assay in the MDA-MB-231 cell line for 24, 48, and 72 hours. No obvious cytotoxicity was observed for chelidonine-free PLGA NPs at various concentrations. Both FCM and CM-PLGA NPs exhibited dose and time-dependent cytotoxicity. The anti-proliferative effect of CM-PLGA NPs was significantly more than FCM at the same concentrations and incubation time (Figure 5).

Higher values of IC-50 (Table 2), as the drug inhibitory concentration required to cause 50% of tumor cell death in a certain period, was obtained for FCM compared with CM-PLGA NPs, which confirms more cytotoxic effects of drug-loaded NPs.

Discussion
The significant cytotoxic activity of chelidonine against various human cancer cells is explained in literature data. However, chelidonine is extremely hydrophobic, which is the major obstacle to successful treatment.

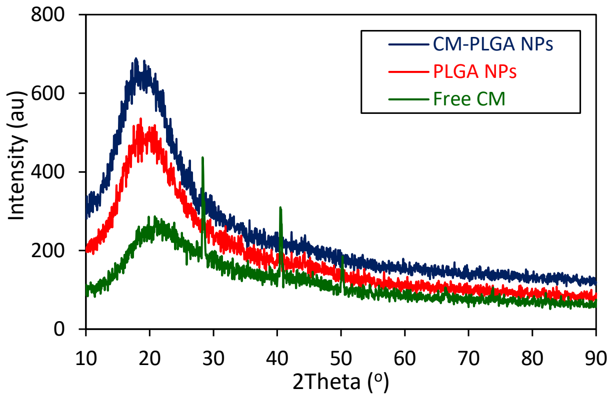

Figure 3. X-ray diffraction patterns of PLGA NPs, free chelidonine (FCM), and chelidonine loaded PLGA (CM-PLGA) NPs. PLGA: Poly(lactic-co-glycolic acid); NPs: Nanoparticles.

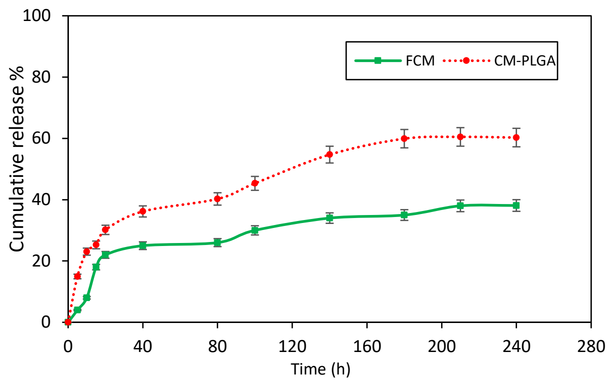

Figure 4. *In vitro* cumulative release for free chelidonine (FCM) and chelidonine-loaded PLGA (CM-PLGA) NPs. Data represent the mean of 3 repeats for each formulation (Mean ± SD). PLGA: Poly(lactic-co-glycolic acid); NPs: Nanoparticles.

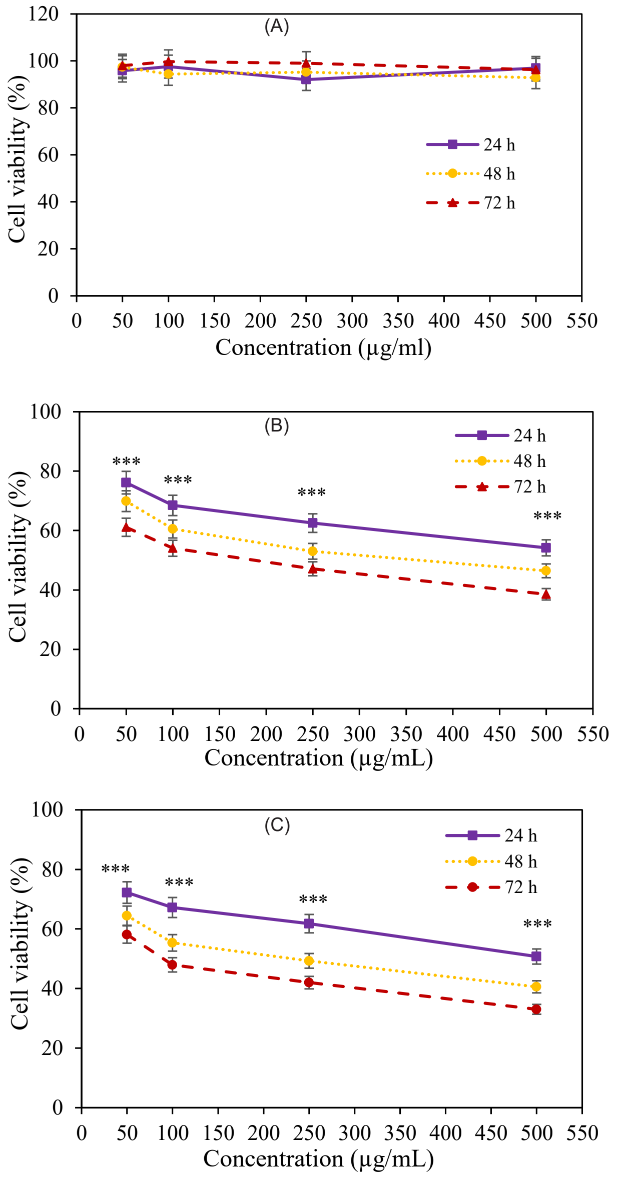

Figure 5. Viability of MDA-MB-231 cells treated with the 50, 100, 250, and 500 µg/mL of (A) PLGA NPs, (B) free chelidonine (FCM), and (C) chelidonine loaded PLGA (CM-PLGA) NPs after 24 h, 48 h, and 72 h treatment (n=3, **P* value < 0.001). PLGA: Poly(lactic-co-glycolic acid); NPs: Nanoparticles.

Whereas not much investigation has been done to overcome this issue, this study was carried out in order to improve chelidonine bioavailability without influencing its biological properties. Physicochemical characters affect the fate of the polymeric NPs. Present findings indicated that NPs were successfully prepared by a single emulsion technique in the nanometer scale. Particle size is considered an important factor in drug delivery systems because it affects the pharmaceutical properties of the drug, including the release profile and cellular uptake of the therapeutic agents. PDI values showed a narrow distribution of NPs, which suggests that the presence of PVA could be able to form a homogeneous nanoparticle dispersion (10). The high drug loading and entrapment efficiency ensured the successful preparation of chelidonine-loaded PLGA nanoformulations. This might be due to the strong interaction between chelidonine as a hydrophobic drug and a hydrophobic polymeric matrix (13). The zeta potential determines the surface charge of NPs, which can influence the particle stability and the fate of NPs in the systemic circulation. The zeta potential of nanoformulations was negative, probably due to the carboxylic groups of PLGA (14). Despite the negative absolute value of the zeta potential of NPs reducing undesirable clearance by the reticuloendothelial system (RES) and increasing their half-life in blood circulation, positively charged NPs have a higher rate of cellular uptake due to the negatively charged cell membrane (15). The tendency of the small particles to aggregate during storage leads to a decrease in therapeutic efficacy. The stability test showed that dried particles appeared to be stable without any collapse or shrinkage (16). No significant change was observed in the stability studies confirming the stability and efficacy of chelidonine nano-formulation over a long time for cancer therapy (17). The FTIR analysis revealed no chemical interaction between the PLGA, chelidonine, and surfactant (PVA), which ensures that chelidonine can be entrapped in the NPs without altering its natural structure. The XRD patterns confirmed the crystalline nature of chelidonine, whereas the absence of peaks for PLGA NPs indicated the amorphous nature. The disappearance of the peaks in the drug-loaded formulations suggests that the drug presents in the amorphous phase within the NPs. This indicates that during encapsulation, the drug will be dissolved or dispersed in an organic solvent and may alter its state to amorphous (18). *In vitro* drug release profile exhibited the burst release, which may be attributed to the chelidonine loosely adsorbed on the surface of the particles, whereas sustained release may be attributed to the diffusion, erosion, and degradation of the polymeric matrix (19). It seems that the diffusion mechanism is responsible for the initial release stages for PLGA-based formulation whereas, degradation or erosion controls the final stages of the release (20). The small size nanometric and amorphous nature of nano-formulations increases water permeation in contact with the external aqueous phase, leading to a higher and faster release (21). As the therapeutic efficacy of the drug is strongly influenced by the concentration and duration of drug availability at the tumor site, the sustained release phase observed

Table 2. IC50 values of free chelidonine (FCM) and chelidonine loaded PLGA (CM-PLGA) NPs and on MDA-MB-231 cells following 24, 48, and 72 h treatment

	IC50 (µg/mL)	
Time (h)	CM	CM-PLGA
24	386.46 ± 1.17	341.19 ± 1.17
48	242.66±1.18	181.97± 1.18
72	160.32±1.19	120.23 ± 1.17

PLGA: Poly(lactic-co-glycolic acid); NPs: Nanoparticles.

indicates the use of PLGA NPs as a suitable carrier for tumor targeting leads to sustaining chelidonine prolonged therapeutic effects (8).

Blank PLGA NPs exhibited no cytotoxic effect ensuring that the polymer was safe and non-toxic (22). The lower IC50 values for CM-loaded NPs drug against cellular proliferation is probably attributed to the small size of nanoformulations, which affect their cellular internalization preferentially via the EPR effect (23) leading to high cellular uptake.

Conclusion

In this study, chelidonine-loaded PLGA NPs were successfully prepared by a single emulsion solvent evaporation method. The higher and faster release of encapsulated chelidonine as well as higher cytotoxic effect on MDA-MB-231 cells proved that chelidonine-loaded PLGA nanoformulations would be a better candidate in therapeutic oncology. As many concerns still exist, future studies seem to be required on in vivo animal models to evaluate the effect of this well-known herbal molecule as a therapeutic agent in clinical applications.

Authors' contributions

NT and ZH had a contribution in chemical experiments for the preparation and characterization of NPs. RM and ZH had a role in cell culture experiments and statistical analysis. KS designed the main idea and conducted the research. KS and ZH had a contribution to writing the manuscript and journal submission. All authors read and approved the final version of the manuscript.

Conflict of interests

There is no conflict of interest associated with this study.

Ethical considerations

Ethical issues, including plagiarism, falsification, misconduct, data fabrication, double publication, or redundancy have been carefully observed by authors. The ethical committee of the Islamic Azad University of Najafabad confirmed the protocol (IR.IAU.NAJAFABAD.REC.1397.006).

Funding/Support

This research did not receive any specific grant from funding agencies in the public, commercial, or profit sectors. There has been no financial support for this work.

References

1. Anjum F, Razvi N, Masood MA. Breast cancer therapy: a mini review. MOJ Drug Des Develop Ther. 2017;1(2):35-38. doi: 10.15406/mojddt.2017.01.00006.
2. Abdel-Moneim A, Magdy A. Review on medicinal plants as potential sources of cancer prevention and treatment. Eur J Biomed Pharm Sci. 2016;3(6):45-62.
3. Khan T, Ali M, Khan A, Nisar P, Jan SA, Afridi S, et al. Anticancer plants: a review of the active phytochemicals, applications in animal models, and regulatory aspects. Biomolecules. 2019;10(1):47. doi: 10.3390/biom10010047.
4. Poonam S, Chandana M. A review on anticancer natural drugs. Int J PharmTech Res. 2015;8(7):131-41.
5. El-Readi MZ, Eid S, Ashour ML, Tahrani A, Wink M. Modulation of multidrug resistance in cancer cells by chelidonine and *Chelidonium majus* alkaloids. Phytomedicine. 2013;20(3-4):282-94. doi: 10.1016/j.phymed.2012.11.005.
6. Miraj S. Ethnobotanical study and pharmacological properties of *Chelidonium majus*. Der Pharma Chem. 2016;8(14):216-22.
7. Kim O, Hwangbo C, Kim J, Li DH, Min BS, Lee JH. Chelidonine suppresses migration and invasion of MDA-MB-231 cells by inhibiting formation of the integrin-linked kinase/PINCH/α-parvin complex. Mol Med Rep. 2015;12(2):2161-8. doi: 10.3892/mmr.2015.3621.
8. Paul A, Das S, Das J, Samadder A, Khuda-Bukhsh AR. Cytotoxicity and apoptotic signalling cascade induced by chelidonine-loaded PLGA nanoparticles in HepG2 cells *in vitro* and bioavailability of nano-chelidonine in mice in vivo. Toxicol Lett. 2013;222(1):10-22. doi: 10.1016/j.toxlet.2013.07.006.
9. Khan I, Gothwal A, Sharma AK, Kesharwani P, Gupta L, Iyer AK, et al. PLGA nanoparticles and their versatile role in anticancer drug delivery. Crit Rev Ther Drug Carrier Syst. 2016;33(2):159-93. doi: 10.1615/CritRevTherDrugCarrierSyst.2016015273.
10. Paul A, Bishayee K, Ghosh S, Mukherjee A, Sikdar S, Chakraborty D, et al. Chelidonine isolated from ethanolic extract of *Chelidonium majus* promotes apoptosis in HeLa cells through p38-p53 and PI3K/AKT signalling pathways. Zhong Xi Yi Jie He Xue Bao. 2012;10(9):1025-38. doi: 10.3736/jcim20120912.
11. Dinarvand R, Sepehri N, Manoochehri S, Rouhani H, Atyabi F. Polylactide-co-glycolide nanoparticles for controlled delivery of anticancer agents. Int J Nanomedicine. 2011;6:877-95. doi: 10.2147/ijn.s18905.
12. Sharma S, Parmar A, Kori S, Sandhir R. PLGA-based nanoparticles: a new paradigm in biomedical applications. TrAC Trends Anal Chem. 2016;80:30-40. doi: 10.1016/j.trac.2015.06.014.
13. Yallapu MM, Gupta BK, Jaggi M, Chauhan SC. Fabrication of curcumin encapsulated PLGA nanoparticles for improved therapeutic effects in metastatic cancer cells. J Colloid Interface Sci. 2010;351(1):19-29. doi: 10.1016/j.jcis.2010.05.022.
14. Khayata N, Abdelwahed W, Chehna MF, Charcosset C, Fessi H. Preparation of vitamin E loaded nanocapsules by the nanoprecipitation method: from laboratory scale to large scale using a membrane contactor. Int J Pharm. 2012;423(2):419-27. doi: 10.1016/j.ijpharm.2011.12.016.
15. Jain AK, Das M, Swarnakar NK, Jain S. Engineered PLGA nanoparticles: an emerging delivery tool in cancer therapeutics. Crit Rev Ther Drug Carrier Syst. 2011;28(1):1-45. doi: 10.1615/critrevtherdrugcarriersyst.v28.i1.10.
16. Das S, Suresh PK. Nanosuspension: a new vehicle for the improvement of the delivery of drugs to the ocular surface. Application to amphotericin B. Nanomedicine.

2011;7(2):242-7. doi: 10.1016/j.nano.2010.07.003.
17. Zhou H, Qian H. Preparation and characterization of pH-sensitive nanoparticles of budesonide for the treatment of ulcerative colitis. Drug Des Devel Ther. 2018;12:2601-9. doi: 10.2147/dddt.s170676.
18. Khanal S, Adhikari U, Rijal NP, Bhattarai SR, Sankar J, Bhattarai N. pH-responsive PLGA nanoparticle for controlled payload delivery of diclofenac sodium. J Funct Biomater. 2016;7(3):21. doi: 10.3390/jfb7030021.
19. Gaonkar RH, Ganguly S, Dewanjee S, Sinha S, Gupta A, Ganguly S, et al. Garcinol loaded vitamin E TPGS emulsified PLGA nanoparticles: preparation, physicochemical characterization, *in vitro* and in vivo studies. Sci Rep. 2017;7(1):530. doi: 10.1038/s41598-017-00696-6.
20. Kızılbey K. Optimization of rutin-loaded PLGA nanoparticles synthesized by single-emulsion solvent evaporation method. ACS Omega. 2019;4(1):555-62. doi: 10.1021/acsomega.8b02767.
21. Mittal G, Sahana DK, Bhardwaj V, Ravi Kumar MN. Estradiol loaded PLGA nanoparticles for oral administration: effect of polymer molecular weight and copolymer composition on release behavior *in vitro* and in vivo. J Control Release. 2007;119(1):77-85. doi: 10.1016/j.jconrel.2007.01.016.
22. Ma Y, Zheng Y, Liu K, Tian G, Tian Y, Xu L, et al. Nanoparticles of poly(lactide-co-glycolide)-d-a-tocopheryl polyethylene glycol 1000 succinate random copolymer for cancer treatment. Nanoscale Res Lett. 2010;5(7):1161-9. doi: 10.1007/s11671-010-9620-3.
23. Honary S, Zahir F. Effect of zeta potential on the properties of nano-drug delivery systems-a review (Part 1). Trop J Pharm Res. 2013;12(2):255-64. doi: 10.4314/tjpr.v12i2.19.